The EMBO Journal (2007) 26, 3783–3793 | © 2007 European Molecular Biology Organization | Some Rights Reserved 0261-4189/07
www.embojournal.org

THE EMBO JOURNAL

EMBO open

In vivo analysis of cohesin architecture using FRET in the budding yeast *Saccharomyces cerevisiae*

John Mc Intyre[1], Eric GD Muller[2], Stefan Weitzer[1,3], Brian E Snydsman[2], Trisha N Davis[2] and Frank Uhlmann[1,*]

[1]Chromosome Segregation Laboratory, Cancer Research UK London Research Institute, London, UK and [2]Department of Biochemistry, University of Washington, Seattle, WA, USA

Cohesion between sister chromatids in eukaryotes is mediated by the evolutionarily conserved cohesin complex. Cohesin forms a proteinaceous ring, large enough to trap pairs of replicated sister chromatids. The circumference consists of the Smc1 and Smc3 subunits, while Scc1 is thought to close the ring by bridging the Smc (structural maintenance of chromosomes) ATPase head domains. Little is known about two additional subunits, Scc3 and Pds5, and about possible conformational changes of the complex during the cell cycle. We have employed fluorescence resonance energy transfer (FRET) to analyse interactions within the cohesin complex in live budding yeast. These experiments reveal an unexpected geometry of Scc1 at the Smc heads, and suggest that Pds5 plays a role at the Smc hinge on the opposite side of the ring. Key subunit interactions, including close proximity of the two ATPase heads, are constitutive throughout the cell cycle. This depicts cohesin as a stable molecular machine undergoing only transient conformational changes during binding and dissociation from chromosomes. Using FRET, we did not observe interactions between more than one cohesin complex *in vivo*.

The EMBO Journal (2007) **26,** 3783–3793. doi:10.1038/sj.emboj.7601793; Published online 26 July 2007
Subject Categories: chromatin & transcription; cell cycle
Keywords: chromosome segregation; cohesin; FRET; *S. cerevisiae*; Smc proteins

Introduction

Cohesin is member of the family of Smc (structural maintenance of chromosomes) containing protein complexes. Smc complexes are conserved from prokaryotes and archea to eukaryotes, and play important roles in chromosome structure and segregation in all organisms studied (Nasmyth and Haering, 2005; Hirano, 2006). Eukaryotes contain at least three distinct Smc complexes that have partly overlapping functions, but each of which is essential for cell viability. The cohesin complex associates with chromosomes during G1 phase of the cell cycle, and ensures that the sister chromatids produced during DNA replication in S-phase remain paired with each other after their synthesis. This pairing allows recognition of the replication products in mitosis by the spindle apparatus and their bipolar alignment on the mitotic spindle. Cleavage of the cohesin subunit Scc1 by the protease separase liberates sister chromatids to trigger chromosome segregation at anaphase onset. The other Smc complexes are condensin, required for chromosome compaction during mitosis, and an Smc5/Smc6 containing complex with a role in DNA repair. Smc complexes are involved in several additional aspects of chromosome biology, including transcriptional regulation, chromatin boundary formation, and the DNA replication checkpoint. The mechanistic basis by which Smc complexes act on chromosomes is still poorly understood.

Cohesin forms a large proteinaceous ring whose circumference is largely composed of the coiled coils of the Smc1 and Smc3 subunits. Electron micrographs of vertebrate cohesin illustrate the ring shape, and interaction studies with recombinant subunits expressed in baculovirus-infected insect cells have demonstrated the subunit arrangement to form this ring (Anderson *et al*, 2002; Haering *et al*, 2002). It is thought that the cohesin ring binds to chromosomes by topologically embracing DNA (Ivanov and Nasmyth, 2005). Mutant analysis *in vivo* has furthermore suggested that ATP bound to the Smc head domains must be hydrolysed for cohesin to load onto chromosomes (Arumugam *et al*, 2003; Weitzer *et al*, 2003). Cohesin associates with chromosomes initially at sites bound by the Scc2/Scc4 cohesin loader, an essential cofactor in the loading reaction. From these sites, cohesin appears to translocate away towards sites of convergent transcriptional termination (Ciosk *et al*, 2000; Lengronne *et al*, 2004).

How DNA enters the cohesin ring, and what effect binding and hydrolysis of ATP has on the conformation of the complex is poorly understood. Recent results suggest that in addition to the ATPase heads the Smc hinge, where Smc1 and Smc3 interact at the opposite side of the ring, plays an important role in DNA binding of Smc complexes (Gruber *et al*, 2006; Hirano and Hirano, 2006; Milutinovich *et al*, 2007). In particular, it has been suggested that the interface between Smc1 and Smc3 at the hinge may need to open up to let DNA enter the ring. How energy derived from ATP hydrolysis at the heads is transferred to open up the hinge is unclear. Atomic force microscopic images of both the fission yeast condensin complex, as well as the cohesin Smc1/3 dimer, have shown that the Smc hinge bends back towards the heads (Yoshimura *et al*, 2002; Sakai *et al*, 2003), but biochemical confirmation of a possible head–hinge inter-

*Corresponding author. Chromosome Segregation Laboratory, Cancer Research UK London Research Institute, 44 Lincoln's Inn Fields, London WC2A 3PX, UK. Tel.: +44 207 269 3024; Fax: +44 207 269 3258; E-mail: frank.uhlmann@cancer.org.uk
[3]Present address: Institute of Molecular Biotechnology, 1030 Vienna, Austria

Received: 16 March 2007; accepted: 18 June 2007; published online: 26 July 2007

action is missing. Once chromosome-bound, cohesin's behaviour during DNA replication, when it links the nascent sister chromatids, is also poorly understood. An ATPase motif that is important during binding of cohesin to chromosomes in G1 is no longer required (Lengronne *et al*, 2006). How therefore the two replication products are trapped by cohesin, is not known. The replication fork might pass through the cohesin ring, leaving replication products trapped inside, without participation of cohesin's ATPase. In addition, binding of cohesin to human chromosomes becomes more stable at the time of S-phase (Gerlich *et al*, 2006). It has remained controversial whether after replication individual cohesin complexes embrace both sister chromatids, or whether interactions between more than one cohesin complex establish sister chromatid cohesion.

The geometry of the cohesin complex bound to chromosomes *in vivo*, and possible conformational changes during DNA binding and the establishment of sister chromatid cohesion, are difficult to study using conventional biochemical techniques. As a step towards addressing these questions, we have analysed fluorescence resonance energy transfer (FRET) between cyan fluorescent protein (CFP) and yellow fluorescent protein (YFP) fluorophores fused to cohesin subunits in live budding yeast. This allows determination of relative distances between the fluorophores and their possible changes during the cell cycle. Systematic FRET measurements between pairwise fluorophore combinations allowed us to refine the picture of the complex and place Pds5 as a possible matchmaker between opposite sides of the complex. Our results suggest a stable geometry of cohesin throughout the cell cycle, and that any conformational changes in response to ATP hydrolysis are likely to be transient. We also used FRET to search for interactions between more than one cohesin complex. Together, this allows us to present an updated view on the behaviour of the cohesin complex *in vivo*.

Results

Measurement of FRET between cohesin subunits

To analyse FRET between cohesin subunits *in vivo*, we utilised a recently developed simple and robust method based on the FRET ratio ($FRET_R$; Muller *et al*, 2005). In this approach, fluorescent intensities of CFP and YFP are measured with an epifluorescent microscope, and FRET is seen after excitation of the CFP fluorophore as increased emission in the YFP channel. Even without FRET, fluorescence is detected after CFP illumination in the YFP channel due to spectral spillover between the channels. Therefore, spillover factors are first determined, and $FRET_R$ is measured as the ratio of the observed FRET intensity over the expected spillover (see Materials and methods, and Muller *et al*, 2005, for details).

$FRET_R$ gives a measure for FRET that is independent of fluorophore concentration, but sensitivity of the measurements is greatest for equimolar fluorophore concentrations. We therefore compared the concentration of the cohesin subunits within budding yeast by measuring fluorescent intensities of CFP fusions expressed at their genomic loci. For these, and all following experiments, we used homozygous diploid yeast strains, which yield increased fluorescent intensities over haploid strains. *ADE3* was deleted and the growth medium supplemented with adenine to reduce background fluorescence from intermediates of the adenine biosynthesis pathway. All cohesin subunits are essential genes in budding yeast, and the fluorophore-tagged subunits in all cases were the only copies of the proteins present in the cells analysed. There were no growth defects, indicating that the tagged proteins were all functional in sustaining all essential aspects of cohesin activity. Fluorescence intensities were measured in an area of fixed size within the nucleus of all strains containing the cohesin subunit-CFP fusions (Figure 1A and Supplementary Figure S1). This showed that in budded G2 cells, all cohesin subunits were present at approximately the same concentration. Approximately 5000 copies of cohesin are present in haploid G2 cells (Ghaemmaghami *et al*, 2003; Weitzer *et al*, 2003), and we expect approximately double this number in our diploid strains.

While observing fluorophore-tagged cohesin subunits, we noticed that in cells with small to medium-sized buds cohesin was enriched in a distinct focus within the nucleus. At higher resolution, the focus appeared to acquire the shape of a ring. Dual-colour imaging, including spindle pole body (SPB) and kinetochore markers, showed that the foci likely represent centromeres, clustered around the SPB, where cohesin is enriched (Supplementary Figure S2) (Guacci *et al*, 1997; Blat and Kleckner, 1999). While centromeres remain attached to the SPB throughout the cell cycle, the timing of foci appearance correlated well with cohesin binding to chromosomes, from the G1/S transition when buds emerge until in mitosis. In early-anaphase nuclei, when cohesin dissociates from chromosomes after Scc1 cleavage, the foci disappeared. Between anaphase and G1, most subunits appeared diffuse throughout the nucleus. As an exception, Scc3-CFP was enriched along the nuclear membrane during this time, but we do not know the reason or possible consequence of this (Supplementary Figure S1).

Because of the greater signal intensities, the fluorescence intensity measurements above were made within the nuclear foci. FRET measurements in G2 cells were also routinely made within the foci. Analyses within the diffuse nuclear region that were performed in parallel gave similar results (Supplementary Figure S3). As a positive control for FRET we attached a tandem fusion of CFP with YFP, separated by a short glycine–alanine linker, to the C-termini of both Scc3 and Pds5. $FRET_R$ for these strains was 2.15 ± 0.2 ($n = 32$) and 2.12 ± 0.24 ($n = 34$) (Figure 1B). This provides an upper limit for $FRET_R$ expected from closely juxtaposed CFP and YFP fluorophores. If there is no FRET between CFP and YFP, the signal intensity in the FRET channel is expected to be equal to the spillover from both fluorophores, resulting in a $FRET_R$ value of 1. Values close to this negative baseline were observed, for example, when the C-terminal Scc3-CFP tag was combined with Pds5-YFP, $FRET_R$ had a value 1.07 ± 0.09 ($n = 52$), or vice versa Scc3-YFP with Pds5-CFP, $FRET_R$ had a value 0.99 ± 0.14 ($n = 31$).

Constitutive close interaction of Smc1 and Smc3 heads

Of particular interest within the cohesin complex are the two Smc ATPase head domains. The Smc ATPase is part of the family of 'ATP binding cassette (ABC)' ATPases, whose function is thought to involve ATP-dependent dimerisation. Structural and biochemical analysis of the Rad50 ABC ATPase has shown how ATP is sandwiched between the two head domains to promote their dimerisation (Hopfner

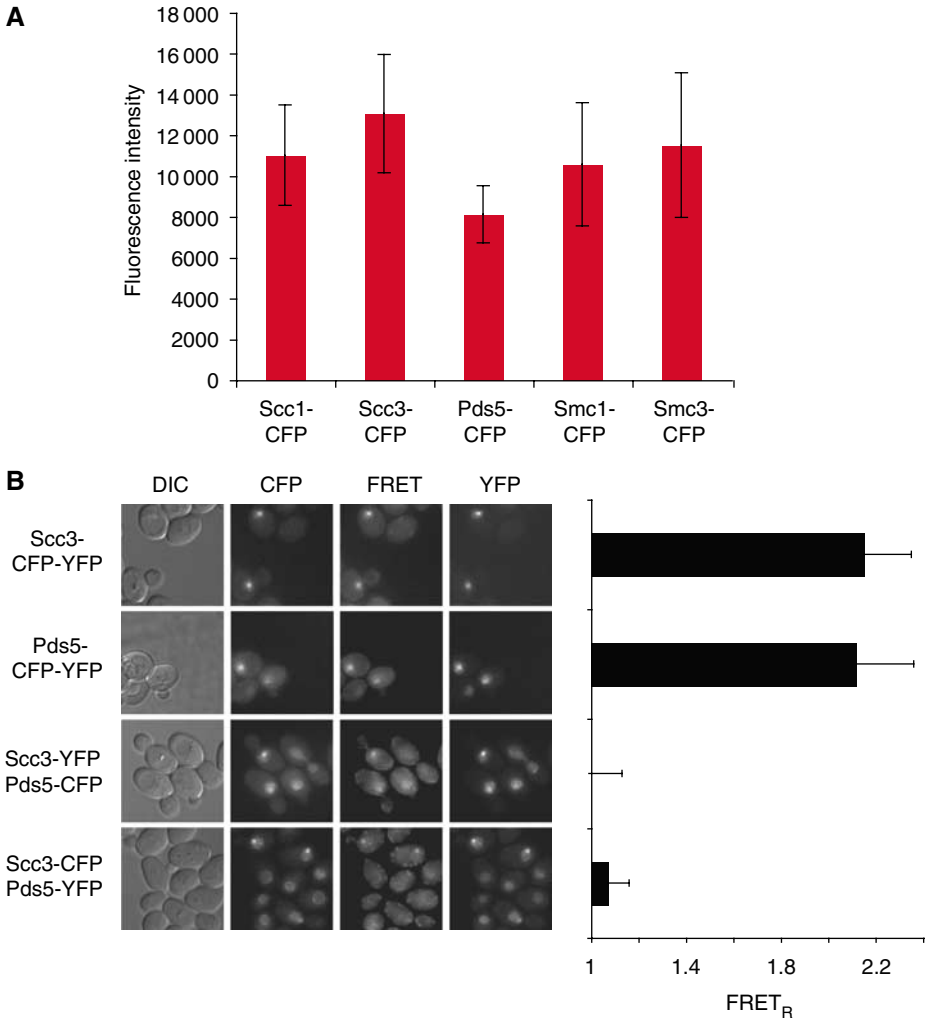

Figure 1 Establishment of FRET to analyse proximity between cohesin subunits in budding yeast. (**A**) *In vivo* concentrations of five budding yeast cohesin subunits. Nuclear fluorescence intensities were measured in yeast strains Y3087 (*MAT*a/α *SCC1-CFP)*, Y2490 (*MAT*a/α *SCC3-CFP*), Y2489 (*MAT*a/α *PDS5-CFP)*, Y1967 (*MAT*a/α *SMC1-CFP*) and Y1971 (*MAT*a/α *SMC3-CFP*). Error bars represent s.d. ($n \geqslant 50$ for each strain). (**B**) Positive and negative FRET controls. Strains Y2588 (*MAT*a/α *SCC3-YFP-CFP*) and Y2587 (*MAT*a/α *PDS5-YFP-CFP*) were subject to FRET analysis. Fluorescence in the YFP, FRET and CFP channels is shown, as well as the $FRET_R$ values derived, as described in Materials and methods. Strains containing fluorophore pairs at the Scc3 and Pds5 C-termini, Y2575 (*MAT*a/α *SCC3-YFP PDS5-CFP*) and Y2574 (*MAT*a/α *SCC3-CFP PDS5-YFP*), showed fluorescence intensities in the FRET channel close to what is expected from spectral spillover alone.

et al, 2001). Crystal structures of bacterial Smc heads, and of the budding yeast Smc1 head bound to ATP, suggest that they use a similar mode of ATP-dependent dimerisation (Haering *et al*, 2004; Lammens *et al*, 2004). It is unknown, however, when during the cell cycle cohesin ATPase heads dimerise or dissociate. Interaction studies have suggested that Smc1 and Smc3 heads can bind each other directly, but also that Scc1 might play an important role in bridging or stabilising their interaction. Electron micrographs of cohesin show the Smc head domains separated from each other, bridged by the non-Smc subunits (Anderson *et al*, 2002; Haering *et al*, 2002; Gruber *et al*, 2003; Weitzer *et al*, 2003).

To examine the interaction between the Smc heads *in vivo*, we measured FRET between Smc1 and Smc3 tagged at their C-termini with YFP and CFP, respectively. $FRET_R$ in budded exponentially growing cells was 2.06 ± 0.14 ($n = 38$; Figure 2A). This value is close to $FRET_R$ observed for the covalent CFP-YFP fusion controls, indicating close proximity between the Smc heads. Exchanging the tags (i.e., Smc1-CFP, Smc3-YFP) produced similar results ($FRET_R = 2.12 \pm 0.19$, $n = 47$). We next asked whether the close association of the Smc heads was regulated during the cell cycle, and if it depended on Scc1. We monitored FRET between Smc1-CFP and Smc3-YFP after release of small unbudded G1 cells, obtained by centrifugal elutriation, into progression through the cell cycle (Figure 2B). Thirty minutes after release, cells were still in G1 and the Smc fluorescence diffuse in the nucleus, probably because Scc1 was not yet present. $FRET_R$ was 2.03 ± 0.44, indicating close association of the Smc heads. As cells progressed through S, G2 and M phases, no significant change to $FRET_R$ was observed.

Despite the high $FRET_R$ value, indicating close proximity between the Smc heads, it is difficult to estimate their actual physical distance. The distance between the termini must be less than 10 nm, the limit of FRET between CFP and YFP, and because of the high value is probably closer to 3 nm, the minimum distance between the fluorophores. Because FRET was similarly high in G1, when Scc1 is absent, it is likely that it represents direct dimerisation of the ATPase heads. To confirm that the observed FRET represents direct,

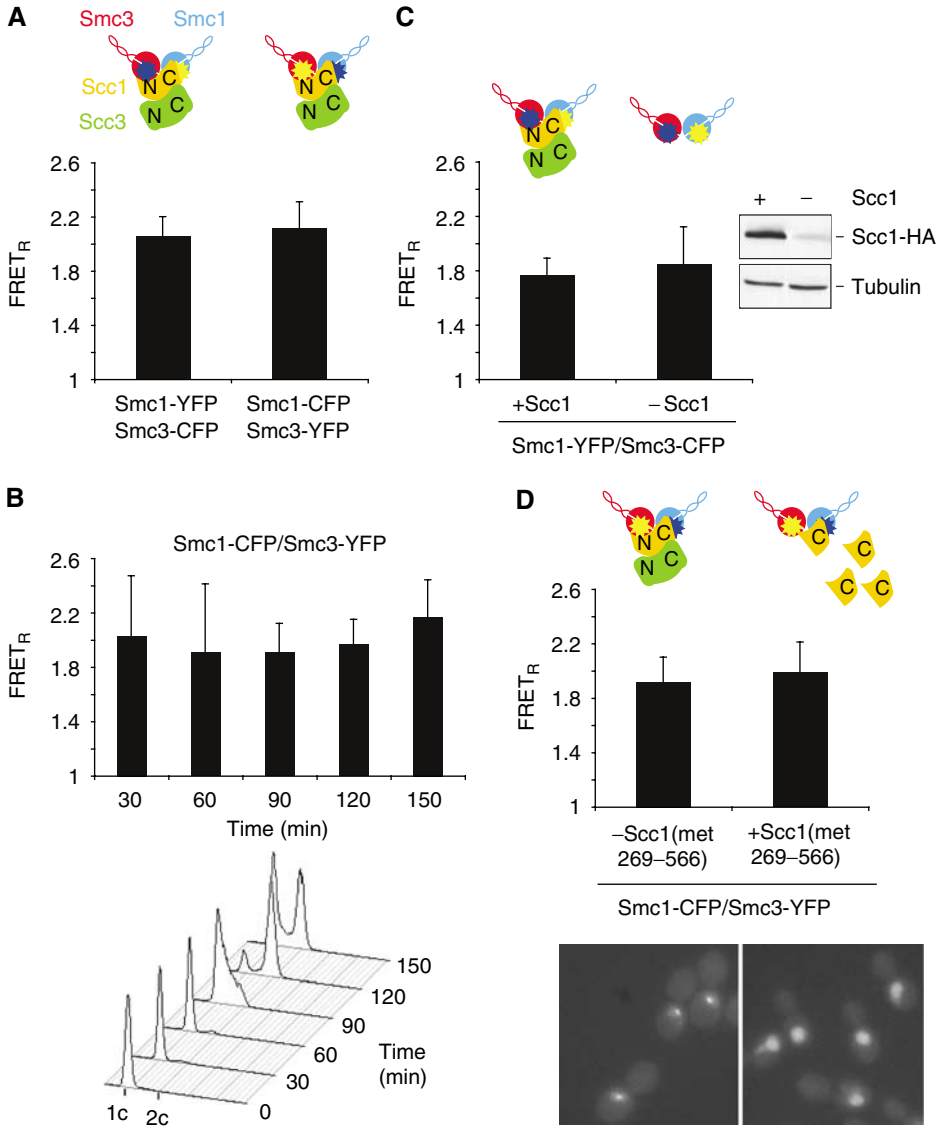

Figure 2 Constitutive proximity of the Smc1 and Smc3 ATPase heads. (**A**) Close proximity of fluorophore pairs attached to the Smc1 and Smc3 heads. FRET was analysed in exponentially growing cells of strains Y1966 (*MAT*a/α *SMC1-YFP SMC3-CFP*) and Y1972 (*MAT*a/α *SMC1-CFP SMC3-YFP*). (**B**) Constitutive Smc1/Smc3 head proximity throughout the cell cycle. Small unbudded G1 cells of strain Y1972 were isolated by centrifugal elutriation and released to progress through a synchronous cell cycle. Samples for FRET analysis were processed every 30 min. Cell cycle progression was monitored by FACS analysis of DNA content. (**C**) Scc1-independent association of the Smc1/Smc3 heads. Strain Y2864 (*MAT*a/α *SMC1-YFP SMC3-CFP GAL1-SCC1-HA3*) was grown in galactose containing medium and one-half of the culture as transferred to medium lacking galactose, to repress Scc1 expression. After 2 h Scc1 levels and FRET were analysed. (**D**) Smc head proximity is maintained after cohesin dissociation from chromosomes. Cells of strain Y3254 (*MAT*a/α *SMC1-CFP SMC3-YFP GAL1-SCC1(met269-566)*) were grown in YP raffinose medium, and arrested in G2/M by nocodazole treatment. Expression of the Scc1 C-terminal fragment was induced by galactose addition for 2 h, and confirmed by Western blotting (data not shown). FRET was analysed in these and control cells that were left without galactose. Images show redistribution of cohesin from nuclear foci after expression of the Scc1 cleavage fragment.

Scc1-independent, association of the Smc heads, we repeated the measurements in cells in the presence of, or depleted for Scc1. For this, we replaced the Scc1 promoter with the galactose-inducible *GAL1* promoter. Cells were grown in medium containing galactose, then the culture was split and one half was transferred to medium lacking galactose to repress Scc1 expression. Two hours later, Scc1 was largely depleted from the culture lacking galactose (Figure 2C). As expected, in the absence of Scc1, cohesin failed to associate with chromosomes, and nuclear foci were not observed (data not shown). FRET between Smc1-CFP and Smc3-YFP was similar with or without Scc1 (with Scc1: $FRET_R = 1.77 \pm 0.12$, $n = 53$; without Scc1: $FRET_R = 1.85 \pm 0.27$, $n = 47$). Note that in this experiment a microscope with greater spectral spillover resulted in lower absolute $FRET_R$ values. These results suggest that the two Smc heads dimerise, probably in an ATP-bound state, in the absence of Scc1, and that they retain close association after Scc1 joins the complex and cohesin is loaded onto chromosomes.

We next analysed whether we could detect Smc head disengagement when Scc1 is cleaved and the cohesin ring dissociates from chromosomes in anaphase. We measured FRET in early anaphase cells displaying dumbbell-shaped nuclei selected from the 120 min time point of the experiment

shown in Figure 2B. Foci of cohesin had dispersed, as expected, but we did not find evidence for a greater distance between the Smc heads ($FRET_R = 1.92 \pm 0.26$, $n = 63$). FRET in our experiments is a population average of all cohesin molecules present in the observation area. Transient, asynchronous dissociation of the Smc heads during cohesin loading or unloading from chromosomes would not be detectable with our technique. Alternatively, ATP hydrolysis during cohesin loading, and Scc1 cleavage in anaphase, may lead to conformational changes in the cohesin complex that do not alter the distance between the fluorophores attached to the Smc1 and Smc3 C-termini.

We next tried to enrich for 'open' cohesin complexes in anaphase by ectopic overexpression of a C-terminal Scc1 cleavage fragment (Scc1(met269-566)). This fragment resembles that normally produced by separase cleavage of Scc1. It associates with the Smc1 head and weakens its interaction with Smc3 (Rao *et al*, 2001; Weitzer *et al*, 2003). Cells were arrested in metaphase by nocodazole treatment, and expression of Scc1(met269-566) induced for 2 h. Nuclear foci disappeared, consistent with cohesin dissociation from chromosomes (Figure 2D). Nevertheless, FRET between the Smc heads did not diminish ($FRET_R = 1.99 \pm 0.22$, $n = 71$), similar to control cells not expressing the Scc1 fragment ($FRET_R = 1.92 \pm 0.18$, $n = 58$). This suggests that even when the interaction between the Smc heads is weakened by the Scc1 cleavage product, they remain associated. The high local concentration of the two heads, connected at the Smc hinge, might promote their association. Weakening of the Smc head interaction may facilitate transient head dissociation during anaphase, too short-lived to be detected under our conditions. Alternatively, Scc1 cleavage may promote another conformational change within cohesin that leads to its removal from chromosomes.

An unexpected geometry of Scc1 at the Smc heads

We next used FRET to study the interaction of Scc1 with the Smc heads. We constructed strains harbouring fluorophores at the Scc1 N- or C-termini, in combination with fluorophores at the Smc heads. In the following, we use YFP-Scc1 to indicate YFP fused to the Scc1 N-terminus, and Scc1-YFP for the fluorophore at the C-terminus. Many current models of the cohesin complex draw Scc1's N- and C-termini in considerable distance from each other, bridging a gap between the Smc1 and Smc3 heads (Nasmyth and Haering, 2005; Hirano, 2006). The Scc1 C-terminus is thought to contact only Smc1, while the N-terminus associates with Smc3. If this arrangement was correct, we would expect strong FRET between fluorophores at the Scc1 C-terminus and Smc1, but weak or no FRET with Smc3. Inversely, we would expect FRET between fluorophores at the Scc1 N-terminus and Smc3, but not Smc1. In contrast to these expectations, we observed equally strong FRET between the Scc1 C-terminus and both Smc1 and Smc3. $FRET_R$ between Scc1-YFP and either Smc1-CFP or Smc3-CFP was 1.87 ± 0.25 ($n = 52$) and 1.86 ± 0.16 ($n = 45$), respectively (Figure 3A). We confirmed this observation after exchanging the fluorophore tags, $FRET_R$ between Scc1-CFP and either Smc1-YFP or Smc3-YFP was 1.88 ± 0.17 ($n = 42$) and 1.93 ± 0.15 ($n = 42$), respectively. This suggests that the Scc1 C-terminus is placed close and equidistant from both Smc1 and Smc3 heads. These results are inconsistent with models in which Scc1 bridges a

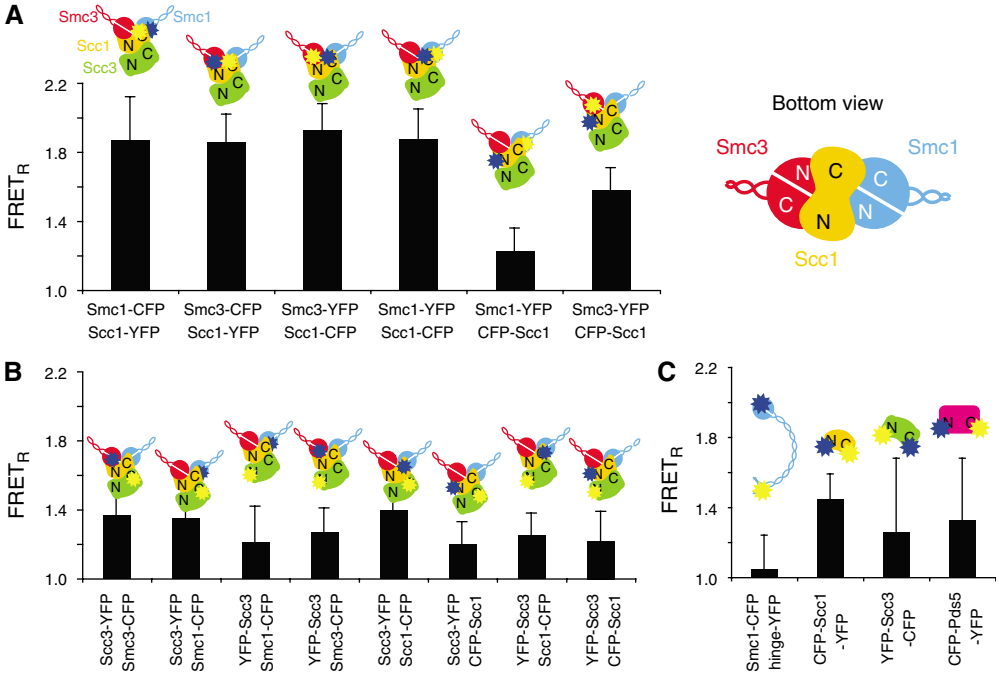

Figure 3 Scc1 and Scc3 association with the cohesin complex. (**A**) An unexpected geometry of Scc1 at the Smc heads. FRET measurements in strains Y2480 (*MATa/α SCC1-YFP SMC1-CFP*), Y2481 (*MATa/α SCC1-YFP SMC3-CFP*), Y2482 (*MATa/α SCC1-CFP SMC3-YFP*), Y2483 (*MATa/α SCC1-CFP SMC1-YFP*), Y2593 (*MATa/α CFP-SCC1 SMC1-YFP*) and Y2594 (*MATa/α CFP-SCC1 SMC3-YFP*) show that the Scc1 C-terminus is placed close and equidistant to both Smc1 and Smc3 heads. A cartoon illustrates the geometry derived from these data. (**B**) Mapping of Scc3 to the cohesin complex. FRET was analysed, from left to right, in strains Y2589, Y2533, Y2721, Y2704, Y2534, Y2591, Y2722 and Y2723. (**C**) Analysis of interactions within cohesin subunits. FRET experiments were performed with strains Y2598 (*MATa/α SMC1hinge-YFP-C-CFP*), Y2592 (*MATa/α CFP-SCC1-YFP*), Y2872 (*MATa/α YFP-SCC3-CFP*) and Y2865 (*MATa/α CFP-PDS5-YFP*).

gap between the Smc heads. Instead they support our finding that the two Smc heads are closely juxtaposed, and suggest that the Scc1 C-terminus is placed between the two heads. The arrangement of the Scc1 C-terminus in its crystal structure with an Smc1 head is consistent with our FRET results (Haering *et al*, 2004), if we consider that Smc3 adopts the position of the second Smc1 head in the homodimer structure.

We next analysed the positioning of the Scc1 N-terminus relative to the Smc heads. $FRET_R$ of CFP-Scc1 with Smc1-YFP or Smc3-YFP was 1.23 ± 0.13 ($n = 49$) and 1.58 ± 0.13 ($n = 48$), respectively. This suggests that the Scc1 N-terminus is positioned closer to the Smc3 head, but that it retains proximity also with Smc1. The association of the Scc1 N-terminus with Smc3 is thought to be less stable than that of the C-terminus with Smc1 (Haering *et al*, 2004). We therefore analysed whether we could see any evidence for a change or regulation of this interaction during the cell cycle. Plotting $FRET_R$ as a function of cell cycle progression showed that the interaction remained constant (Supplementary Figure S4). From these results we suggest that the two Smc heads remain in contact for most of the cell cycle, and that Scc1 binds the two heads in an orientation that is largely perpendicular to the axis that connects the two heads (see schematic representation in Figure 3A).

Scc3's association with the cohesin complex

We next focused our attention on the Scc3 subunit. Biochemical evidence suggests that Scc3 interacts with the Scc1 C-terminal half, and associates with the cohesin complex in an Scc1-dependent manner (Haering *et al*, 2002). To map Scc3 with respect to the other subunits *in vivo*, we carried out FRET experiments with fluorophores attached to either terminus of the subunit. The closest association was found between Scc3-YFP and Scc1-CFP ($FRET_R = 1.4 \pm 0.14$, $n = 44$), consistent with the characterised biochemical interaction (Figure 3B). We also observed FRET between Scc3-YFP and both Smc1-CFP and Smc3-CFP ($FRET_R = 1.35 \pm 0.16$, $n = 55$ and 1.37 ± 0.14, $n = 55$, respectively), suggesting equidistant positioning between the two Smc subunits. Significant FRET also occurred between fluorophores attached to the Scc3 N-terminus and Scc1 or the Smc heads. This confirms association of Scc3 with Scc1 *in vivo*, and suggests that Scc3 is positioned symmetrically with respect to the Smc heads.

Intramolecular FRET within cohesin subunits

We also carried out FRET measurements between intramolecular fluorophore pairs attached to the N- and C-termini of cohesin subunits. This revealed significant FRET between the Scc1 N- and C-termini ($FRET_R = 1.45 \pm 0.14$, $n = 32$), consistent with a relatively close positioning of the two termini with respect to each other within the complex (Figure 3C). We also observed weaker FRET between the tagged N- and C-termini of Scc3 and Pds5, respectively, suggesting that the ends are in relative proximity to each other. We then wanted to probe the geometry of the Smc1 subunit in more detail. The Smc1 head is separated from the Smc hinge by an approximately 50-nm-long stretch of coiled coil. As the Smc hinge has been suggested to show functional interactions with the ATPase heads (Hirano and Hirano, 2006), we assessed the distance between the Smc1 head and hinge by FRET *in vivo*. To this end, we inserted a YFP fluorophore into a predicted surface loop at the Smc1 hinge, and a CFP fluorophore was added to the C-terminus of the same protein. FRET between these fluorophores was close to the negative baseline ($FRET_R = 1.05 \pm 0.19$, $n = 55$). This suggests that a direct interaction between the Smc1 head and hinge, if it exists, only occurs transiently *in vivo*.

Evidence for Scc1-dependent Pds5 association with the Smc hinge

Budding yeast Pds5 is essential for cohesin association with chromosomes, and binds together with cohesin to the same chromosomal sites in late G1 (Hartman *et al*, 2000; Panizza *et al*, 2000; Lengronne *et al*, 2004). Fission yeast and human Pds5 have been shown to be part of the cohesin complex, but appear to be dispensable for a basal level of sister chromatid cohesion (Sumara *et al*, 2000; Tanaka *et al*, 2001; Losada *et al*, 2005). Little is known about the association of Pds5 with cohesin, so we sought to determine with which subunits Pds5 interacts. We failed to detect significant FRET between N- or C-terminal Pds5 fluorophore tags and most cohesin subunits (Figure 4A). Combination of CFP-Pds5 with Scc1-YFP and Pds5-YFP with CFP-Scc1 yielded the highest among the very low $FRET_R$ values ($FRET_R = 1.08 \pm 0.16$, $n = 47$ and $FRET_R = 1.1 \pm 0.13$, $n = 42$, respectively). A *t*-test to evaluate the significance of these values suggested that they are greater than those obtained for the Pds5-YFP/Smc1-CFP pair ($P < 0.01$). These very weak FRET values should be regarded equivocal. To our surprise we found a clear FRET signal between both N- and C-terminally tagged Pds5 and the Smc1 hinge-YFP insertion ($FRET_R = 1.15 \pm 0.23$, $n = 48$ and $FRET_R = 1.21 \pm 0.19$, $n = 40$, respectively, which is greater than the Pds5-YFP/Smc1-CFP pair at $P < 0.0001$). This suggests that Pds5 is in contact with the Smc1 hinge.

Because of the very weak FRET of fluorophore-tagged Pds5 with Scc1, we searched for independent evidence whether Scc1 might be involved in Pds5's interaction with cohesin. We first asked whether an interaction of Pds5 with cohesin can be detected by co-immunoprecipitation. Scc1 co-precipitated with Pds5 from yeast extract and, as has been observed with human cohesin (Sumara *et al*, 2000), this interaction was salt sensitive (Supplementary Figure S5). This confirmed that Pds5 is part of, or interacts with, the budding yeast cohesin complex. We then tested whether the association of Pds5 with cohesin depended on Scc1. Using a strain in which Scc1 could be repressed under control of the *GAL1* promoter, we observed an interaction between Pds5 and the cohesin subunit Smc1 in the presence of Scc1, which was abolished in the absence of Scc1 (Figure 4B). This suggests that the interaction of Pds5 with cohesin depends on Scc1. Pds5 might contact Scc1, and once bound to cohesin, engages in an interaction with the Smc hinge. Alternatively, association of Scc1 with cohesin could introduce a conformational change that allows Pds5 binding to the Smc hinge.

Atomic force microscopy of *Schizosaccharomyces pombe* Smc1/Smc3 heterodimers showed an apparent interaction of the Smc heads with the hinge (Sakai *et al*, 2003), so we wondered whether we could find biochemical evidence for this association. We overexpressed in yeast an Smc1 head construct consisting of the N- and C-terminal head domains connected by a short peptide linker (Weitzer *et al*, 2003), as well as the two Smc1 and Smc3 halves of the hinge. Immunoprecipitation against the Smc1 half-hinge demon-

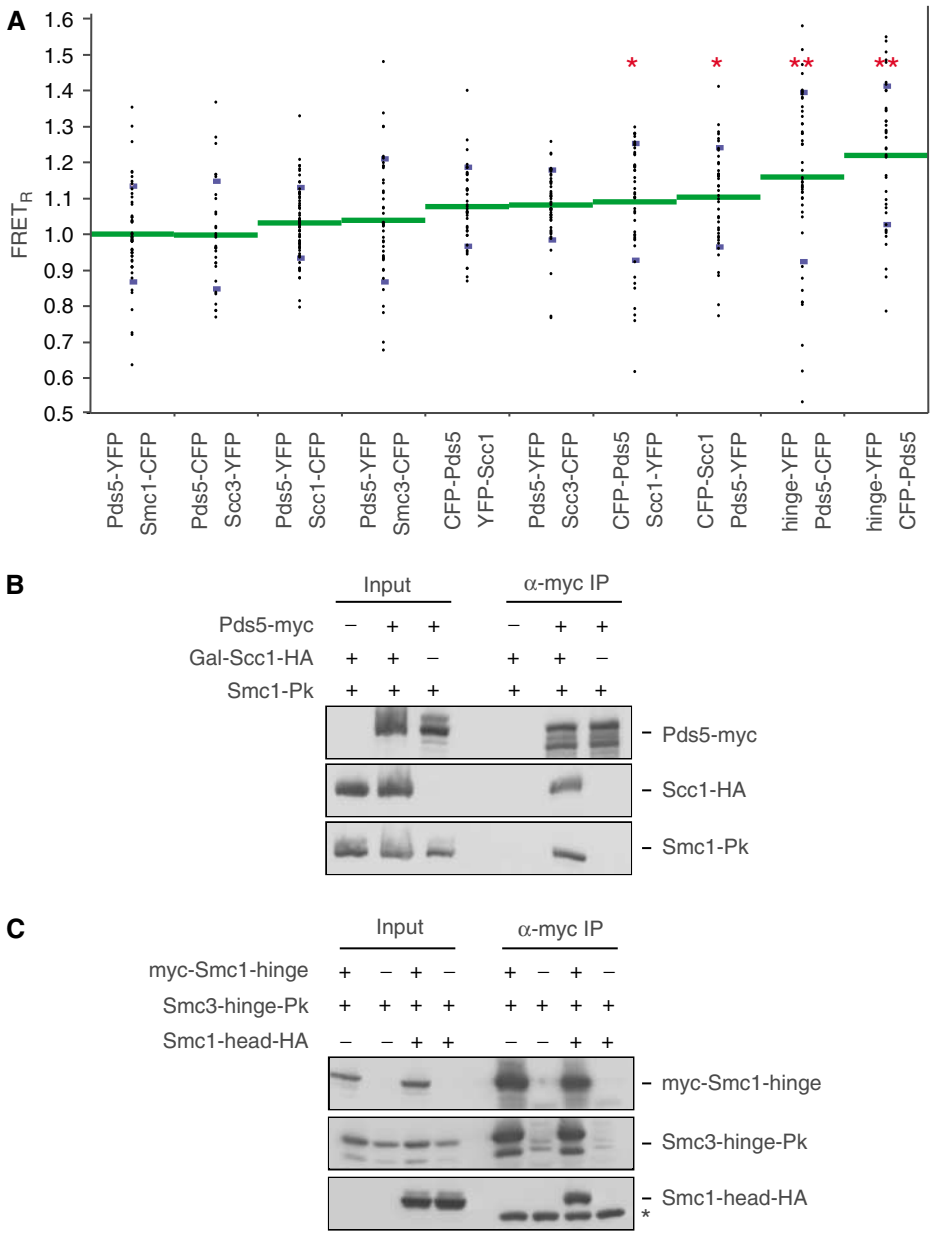

Figure 4 Head–hinge interactions within the cohesin complex. (**A**) Pds5 interaction with both Scc1 and the Smc1 hinge. FRET was measured between fluorophore pairs as indicated, from left to right, in strains Y2531, Y2575, Y2532, Y2530, Y3264, Y2574, Y3275, Y2590, Y2706 and Y2705. Individual measurements are indicated as points, with mean shown as green and s.d. shown as blue lines. $FRET_R$ was significantly different from the Pds5-YFP/Smc1-CFP pair at $*P<0.01$ and $**P<0.0001$, respectively, by Student's *t*-test. (**B**) Scc1-dependent interaction of Pds5 with Smc1. Extracts were prepared from haploid strains Y3223 (*MAT*a *SMC1-Pk3 GAL1-SCC1-HA6*) and Y3210 (as Y3223, but *PDS5-myc18*) in the presence or 2.5 h after repression of Scc1, and co-immunoprecipitation of Smc1 with Pds5 analysed. (**C**) Direct interaction of the Smc1 head and hinge. Protein expression was induced in strains Y2318 (*MAT*a *GAL-SMC3hinge-Pk3 GAL-myc9-SMC1hinge*), Y1823 (*MAT*a *GAL-SMC3hinge-Pk3*), Y2319 (as Y2318, plus *GAL-SMC1head-HA3*) and Y1824 (as Y1823, plus *GAL-SMC1head-HA3*) for 2 h, and protein extracts prepared to analyse co-immunoprecipitation of the Smc1 head and hinge. An asterik indicates the cross-reacting immunoglobulin heavy chain.

strated stable complex formation with the Smc3 part of the hinge (Figure 4C). Moreover, this Smc hinge complex efficiently co-precipitated the Smc1 head, suggestive of a direct head–hinge interaction. The quantities of overexpressed hinge and heads precipitated in this experiment exceeded the level of the endogenous cohesin complex, and we could not detect other cohesin subunits in the immunoprecipitate (data not shown). Therefore, the interaction between the Smc head and hinge observed in this experiment is most likely direct. This evidence for a direct Smc1 head–hinge association is in contrast to our failure to detect physical proximity between the two by FRET *in vivo* (Figure 3C). A possible solution to this apparent paradox is that our biochemical results reveal an interaction that occurs only transiently *in vivo*, either because of a conformational equilibrium biased towards complexes with separated heads and hinge, or because the interaction occurs only as an intermediate, for example, during cohesin loading onto chromosomes.

Interactions between cohesin complexes in vivo

Several models have been put forward to explain how cohesin might link two replication products after DNA

synthesis (Milutinovich and Koshland, 2003; Nasmyth and Haering, 2005; Hirano, 2006; Lengronne *et al*, 2006). One important question is whether one cohesin ring encircles and holds together both sister chromatids, or whether individual cohesin complexes bind both sister chromatids, and linkages are established by interactions between pairs of cohesin complexes. *In vitro* characterisation of cohesin isolated from yeast chromosomes has so far not found evidence for higher order interactions between more than one cohesin complex (Haering *et al*, 2002; Weitzer *et al*, 2003; Ivanov and Nasmyth, 2005). Nevertheless, the existence of such interactions *in vivo* is difficult to exclude. We therefore utilised our FRET assay to search for interactions between two cohesin complexes. We first analysed two copies of Smc1 that were tagged in a diploid yeast strain at their C-termini with CFP and YFP, respectively. The existence of cohesin dimers in 'head to head' orientation should result in FRET between the two tagged Smc1 termini. However, no FRET was detected ($FRET_R = 1.05 \pm 0.24$, $n = 51$) (Figure 5). A similar experiment with CFP- and YFP-tagged copies of Smc3 again detected no interaction ($FRET_R = 1.03 \pm 0.13$, $n = 34$). A corollary of this experiment is that FRET observed between fluorophore-tagged Smc1 and Smc3 is due to head interaction within the cohesin complex, and not due to higher-order cohesin interactions or crowding between adjacent cohesin complexes at chromosomal association sites.

The above experiments would not detect interactions between cohesin complexes if they occurred in a 'hinge to hinge' orientation. To test this possibility, we constructed CFP and YFP insertions within the hinge in the two Smc1 copies of a diploid strain. Again, no FRET was observed ($FRET_R = 1.0 \pm 0.22$, $n = 40$). While these results cannot exclude association between more than one cohesin complex at sites different from the ones here tested, our observations pose limitations on how such interactions could occur *in vivo*.

Discussion

Cohesin analysis using FRET

Cohesin is a ring-shaped multi-subunit protein complex with several intriguing architectural features. Key to cohesin's function *in vivo* are the two Smc ATPase heads that close the ring on one side. Structural and biochemical evidence has been obtained both for direct head–head dimerisation as well as for a role of the Scc1 subunit in bridging a gap between the two heads. Furthermore, structural and functional evidence for an interaction of the Smc heads with the Smc hinge at the opposite side of the ring has been obtained. Which of, and when during cohesin's function in sister chromatid cohesion, these interactions occur *in vivo* remained largely uncharacterised. We have now used FRET to analyse the behaviour of the cohesin complex in live budding yeast.

FRET is a powerful technique to assess the proximity of interacting proteins *in situ*. Recently, a practical method to measure FRET using CFP and YFP fluorophore fusions to budding yeast proteins expressed from their genomic loci *in vivo* has been introduced (Muller *et al*, 2005). In the first instance, this technique was used to obtain a structural image of the core components of the yeast SPB. These measurements were facilitated by the concentration of many copies of each subunit within the small volume of the SPB. We now show that FRET measurements are also possible on a protein complex of moderate abundance and a more dispersed

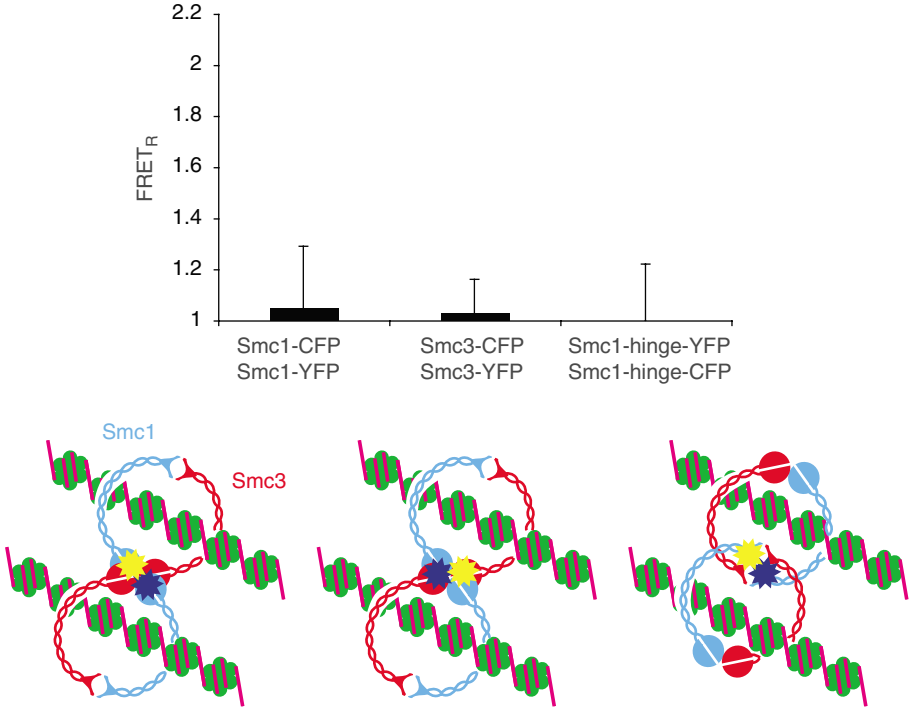

Figure 5 Search for proximity of more than one cohesin complex *in vivo*. FRET measurements to analyse proximity of more than one Smc1 head, Smc3 head or Smc1 hinge, were conducted in strains Y3082 (*MAT*a/α *SMC1-CFP/SMC1-YFP*), Y3083 (*MAT*a/α *SMC3-CFP/SMC3-YFP*) and Y3228 (*MAT*a/α *SMC1hinge-CFP/SMC1hinge-YFP*). The schematic representation illustrates geometries of possible cohesin interactions that have been tested and excluded by this analysis.

localisation in the yeast nucleus. We also use this technique to analyse possible conformational changes in the cohesin complex during the cell cycle. The results have shed new insight into the architecture of cohesin.

In vivo architecture of the cohesin complex

We found that the two ATPase heads are in constitutive close contact with each other throughout the cell cycle. Once synthesised at the G1/S transition, the Scc1 subunit maps to these heads in an unexpected configuration. In contrast to many models in which Scc1 bridges a gap between the Smc heads, we find that the subunit is more likely to lie across two interacting heads, perpendicular to what would be expected from a bridge. Scc1 is predicted to consist of folded domains at the N- and C-termini, connected by less structured central sequences. The N-terminus is thought to contact Smc3, and the C-terminus Smc1. In contrast, our FRET results suggest that the Scc1 C-terminus lies between and equidistant from both Smc heads. This is consistent with crystallographic analysis of the Scc1 C-terminus bound to the Smc1 head (Haering *et al*, 2004), if we assume that Smc3 takes the place of the second Smc1 head in the homodimer crystal structure. Indeed the Scc1 C-terminus is so close to the predicted position of the Smc3 head, that it would be surprising if no contact existed between the two. Interaction studies with recombinant Scc1 fragments and the Smc head domains are not inconsistent with such a notion (Haering *et al*, 2002).

This geometry could have important implications as to the role of Scc1 in the cohesin complex. The observed location of Scc1 is reminiscent of the C-terminal regulatory domain of the MalK ABC transport ATPase (Chen *et al*, 2003). This domain stabilises the interaction between the ATPase heads, while those are undergoing a tweezers-like opening motion. In the case of cohesin, such a motion could be relayed onto the Smc hinge that might contact the ATPase heads opposite to Scc1 from inside the ring. The direct head–hinge interaction that we observe is consistent with this possibility. As suggested, this interaction could mediate opening of the hinge dimer during cohesin loading onto DNA (Gruber *et al*, 2006). The Smc heads might in this way never separate very far, at least until Scc1 is cleaved during anaphase. How exactly Scc1 cleavage leads to cohesin dissociation from chromosomes is not clear. Integrity of Scc1 might be important to mediate its stabilising function between Smc1 and Smc3, and after cleavage, its ability to connect the Smc heads might be disrupted (Gruber *et al*, 2003). An additional, not mutually exclusive, possibility is that the C-terminal cleavage product produced actively interferes with the Smc head interaction, thereby further reducing their affinity (Weitzer *et al*, 2003). While this may well allow the Smc heads to separate and leave DNA to exit the ring during anaphase, our FRET results suggest that separation of the heads even in anaphase, if it occurs, is transient.

We also provide evidence that the Pds5 subunit contacts cohesin in an Scc1-dependent manner, and binds to the Smc hinge at the opposite side of the cohesin ring. This opens the possibility that Pds5 acts as a molecular matchmaker for an interaction between the Smc heads and hinge, as previously seen on atomic force microscopic images (Sakai *et al*, 2003). While we could biochemically demonstrate a robust interaction between the Smc1 head and hinge, this conformation may occur only transiently *in vivo* during the process of DNA binding (Gruber *et al*, 2006; Hirano and Hirano, 2006). Pds5 could facilitate the interaction by bringing together Scc1 and the Smc hinge from opposite sides of the ring. Such a matchmaker role could increase the efficiency of the head–hinge interaction, but may not be essential in all circumstances. This could explain why Pds5 is a dispensable subunit of cohesin in fission yeast, and tolerates reduction by RNA interference in human cultured cells. Pds5 may serve an additional role in maintaining the structural integrity of the cohesin complex during longer periods in G2 (Tanaka *et al*, 2001; Losada *et al*, 2005).

Conformational changes within the cohesin complex

Our analysis of key interactions within cohesin throughout the cell cycle suggested that no major structural changes occur during the binding of cohesin to chromosomes or the establishment of sister chromatid cohesion during S-phase. This is based on constant FRET, when comparing the diffuse nuclear cohesin pool and the nuclear foci enriched in chromosome bound cohesin. It is also based on the analysis of FRET as a function of cell cycle progression. Cohesin binds to chromosomes about 15 min before S-phase, and any significant change to FRET in the course of cohesion establishment during DNA replication should have become detectable. Our results therefore draw the picture of cohesin as a relatively stable molecular machine that undergoes conformational changes only on a transient basis.

The nature of any transient structural changes of the cohesin complex during binding to and dissociation from DNA is of immense interest. Our measurements of population averages of cohesin in the yeast nucleus do not allow detection of such changes. Any conformational change, even if it lasted for a few seconds, long in the time scale of molecular reactions, would go undetected in our measurements. If the total population of cohesin underwent such a change with a synchrony of several minutes, only a low percent of all complexes would be present in an alternative conformation at any one time, an effect too small to be detectable with our technique.

In the future, two advances could allow such reactions to be studied. Ideally, FRET experiments with single molecules in reconstituted DNA binding reactions *in vitro* should allow a more detailed analysis of cohesin's behaviour. This approach is so far limited, in that cohesin loading onto DNA in a purified *in vitro* system has not yet been successfully reconstituted. In the interim, it could become possible to take advantage of the genetic amenability of budding yeast to engineer situations in which cohesin accumulates in intermediates of loading or unloading reactions. This could involve the analysis of mutant cohesin complexes, or of the wild-type complex in different mutant strain backgrounds. In an attempt to trap cohesin during DNA loading, we tried to analyse cohesin in yeast strains mutant for the cohesin loader subunit Scc2 (Ciosk *et al*, 2000; Lengronne *et al*, 2004). However, increased background fluorescence at the higher restrictive temperatures required to inactivate Scc2 prevented us from analysing these strains further. This obstacle could be overcome by the generation of cold-sensitive mutant alleles. The analysis of mutations in cohesin subunit themselves, for example the ATPase motifs, poses a similar challenge. Mutant subunits that do not sustain cell viability have been studied after ectopic expression in addition to the endogenous copy

(Arumugam *et al*, 2003; Weitzer *et al*, 2003). This means that FRET analysis would be limited to a corresponding subset of cohesin complexes with accordingly lower fluorescent and FRET signals. The introduction of more sensitive imaging equipment might open such possibilities in the future.

Our studies so far have provided new insight into the architecture of the cohesin complex *in vivo*, and its behaviour during the cell cycle. Future studies will analyse the mechanism of cohesin, and that of related Smc protein complexes, at higher resolution, to understand their molecular activities in chromosome structure and dynamics.

Materials and methods

Yeast strains and growth conditions

Strains used in this study were diploid, homozygous for all genetic features, unless otherwise stated, and of the W303 background (*MAT*a/α, *ade3*Δ *ade2-1 trp1-1 can1-100 leu2-3,112*, *his3-11*, *ura3-52*). YEP medium was supplemented with either 2% glucose or 2% raffinose. To induce expression from the *GAL1* promoter, YEP + raffinose medium was supplemented with 2% galactose. Arrest in G2/M phase was achieved by addition of the spindle poison nocodazole at 5 μg/ml for 2 h. Small G1 cells were isolated by centrifugal elutriation, as described (Sundberg *et al*, 1996).

Strain construction

N- and C-terminal tagging of genes at their genomic loci was performed by gene targeting using polymerase chain reaction (PCR) products (Wach *et al*, 1994; Prein *et al*, 2000). Details of the YFP and CFP variants, the protocols used, as well as the plasmid templates themselves are available from the University of Washington Yeast Resource Center (http://depts.washington.edu/~yeastrc). To construct a fluorophore insertion at the Smc1 hinge, we predicted surface loops in the hinge region by sequence alignment with the *Thermotoga maritima* Smc hinge, for which a crystal structure has been determined (Haering *et al*, 2002). Of two locations tested, insertion of YFP after proline^{600} yielded a Smc1 hinge-YFP derivative that fully complemented cell growth as the sole source of Smc1. The *Smc1* open reading frame until proline^{600} was cloned using PCR as an *Xma*I/*Sal*I fragment into YIplac128, and fused to a *Sal*I/*Sph*I fragment encoding the remainder of Smc1. Inserted into the *Sal*I site was PCR amplified YFP (or CFP) flanked by linker peptides of the sequence VDGSTG on both sites. Next a 472-bp *Smc1* promoter PCR fragment was added upstream using *Nde*I/*Xma*I sites, and finally an additional 470-bp sequence upstream of the *Smc1* promoter fragment was amplified but cloned behind the *Smc1* open reading frame using *Sph*I and *Nla*III. This construct was linearised by *Sph*I restriction for integration at the *Smc1* locus. Constructs for the expression of an Smc1 head and the Smc1/Smc3 hinge were as described (Weitzer *et al*, 2003). The hinge domains included 50 amino acids of flanking coiled coil sequence.

Protein techniques

Immunoprecipitation was performed by the addition of precleared yeast extracts to α-Pk (clone SV5-Pk1, Serotec)- or α-myc (clone 9E10)-conjugated protein-A–Sepharose beads (Sigma) for 90 min. The beads were extensively washed in extraction buffer EBX (50 mM HEPES/KOH pH 7.5, 100 mM KCl, 2.5 mM $MgCl_2$, 0.25% Triton X-100) containing protease inhibitors. For co-immunoprecipitation of Pds5 with Smc1, the concentration of KCl was reduced to 50 mM. Bound proteins were eluted in SDS–PAGE sample buffer and analysed by Western blotting.

Microscopy

Cells for FRET analysis were grown overnight at 30°C on YPD plates supplemented with 150 μg/ml adenine. Pinhead-sized colonies were scraped from the plate and resuspended in 12 μl SC medium. A 3 μl volume of the cell suspension was mounted on an agarose patch (1% SeaPlaque GTG agarose, Cambrex Bio Science, in SC medium) and covered with a coverslip. Cells were observed on a DeltaVision RT system (Applied Precision) based on an Olympus IX71 microscope. CFP excitation and emission filters used were 440AF21 and 480AF30, YFP excitation and emission filters used were 500AF25 and 545AF35 (the first number indicating the wavelength of maximum transmission and the second the bandwidth of the filters), and the dichroic mirror used was 436-510DBDR (all from Omega Optical). We used an × 100 UPUplan Apochromat (NA = 1.4) objective, and images were captured with a CoolSNAP HQ camera (Roper scientific).

FRET analysis

For every analysis, images of 60–80 fields of cells were captured in the following order: YFP, FRET (i.e., CFP excitation and YFP emission filter), CFP and DIC. Exposure time was 0.4 s, with 2 × 2 binning and a final image size of 512 × 512 pixels. Image analysis was performed using softWoRx (Applied Precision). Signal intensities within 5 × 5 pixel boxes were measured, background was subtracted from an adjacent box outside the nucleus, and the intensity values were further analysed using JMP 5.1 software (SAS Institute).

CFP and YFP spillover factors were measured in strains Y1967 and Y1970, expressing Smc1-CFP and Smc1-YFP, respectively. The CFP spillover factor (*CSF*) is the intensity of the Smc1-CFP signal in the FRET channel, divided by its intensity in the CFP channel, and was found to be 0.34 ± 0.04 ($n = 48$). The similarly derived YFP spillover factor (*YSF*) was 0.09 ± 0.04 ($n = 46$). Spillover factor measurements were repeated throughout the course of our studies and did not change significantly. $FRET_R$ in the experimental strains containing fluorophore pairs was derived from three background-corrected intensity measurements, YFP, FRET and CFP, as follows. First, the total expected spillover in each measurement was calculated using the following equation

$$\text{Spillover}_{\text{total}} = (CSF \times \text{CFP}) + (YSF \times \text{YFP}) \quad (1)$$

This was then used to determine the FRET ratio ($FRET_R$).

$$\text{FRET}_R = \frac{\text{FRET}}{\text{spillover}_{\text{total}}} \quad (2)$$

Supplementary data

Supplementary data are available at *The EMBO Journal* Online (http://www.embojournal.org).

Acknowledgements

We thank Neil McDonald for help with the design of the Smc1 hinge fluorophore insertion, Chris Lehane for cloning the Smc hinges, Rafael Carazo-Salas for advise on microscopy, Karl-Peter Hopfner, Martin Singleton and members of our laboratories for discussions and comments on the manuscript. This work was supported by a Human Frontier Science Program Young Investigator Grant to FU, and by the National Center for Research Resources of the National Institutes of Health Grant P41 RR011823 to TND.

References

Anderson DE, Losada A, Erickson HP, Hirano T (2002) Condensin and cohesin display different arm conformations with characteristic hinge angles. *J Cell Biol* **156:** 419–424

Arumugam P, Gruber S, Tanaka K, Haering CH, Mechtler K, Nasmyth K (2003) ATP hydrolysis is required for cohesin's association with chromosomes. *Curr Biol* **13:** 1941–1953

Blat Y, Kleckner N (1999) Cohesins bind to preferential sites along yeast chromosome III, with differential regulation along arms versus the centric region. *Cell* **98:** 249–259

Chen J, Gang L, Lin J, Davidson AL, Quiocho FA (2003) A tweezers-like motion of the ATP-binding cassette dimer in an ABC transport cycle. *Mol Cell* **12:** 651–661

Ciosk R, Shirayama M, Shevchenko A, Tanaka T, Toth A, Shevchenko A, Nasmyth K (2000) Cohesin's binding to chromosomes depends on a separate complex consisting of Scc2 and Scc4 proteins. *Mol Cell* **5:** 1–20

Gerlich D, Koch B, Dupeux F, Peters J-M, Ellenberg J (2006) Live-cell imaging reveals a stable cohesin–chromatin interaction after but not before DNA replication. *Curr Biol* **16:** 1571–1578

Ghaemmaghami S, Huh W-K, Bower K, Howson RW, Belle A, Dephoure N, O'Shea EK, Weissman JS (2003) Global analysis of protein expression in yeast. *Nature* **425:** 737–741

Gruber S, Arumugam P, Katou Y, Kuglitsch D, Helmhart W, Shirahige K, Nasmyth K (2006) Evidence that loading of cohesin onto chromosomes involves opening of its SMC hinge. *Cell* **127:** 523–537

Gruber S, Haering CH, Nasmyth K (2003) Chromosomal cohesin forms a ring. *Cell* **112:** 765–777

Guacci V, Hogan E, Koshland D (1997) Centromere position in budding yeast: evidence for anaphase A. *Mol Biol Cell* **8:** 957–972

Haering CH, Löwe J, Hochwagen A, Nasmyth K (2002) Molecular architecture of SMC proteins and the yeast cohesin complex. *Mol Cell* **9:** 773–788

Haering CH, Schoffnegger D, Nishino T, Helmhart W, Nasmyth K, Löwe J (2004) Structure and stability of cohesin's Smc1–kleisin interaction. *Mol Cell* **15:** 951–964

Hartman T, Stead K, Koshland D, Guacci V (2000) Pds5p is an essential chromosomal protein required for both sister chromatid cohesion and condensation in *Saccharomyces cerevisiae*. *J Cell Biol* **151:** 613–626

Hirano M, Hirano T (2006) Opening closed arms: long-distance activation of SMC ATPase by hinge–DNA interactions. *Mol Cell* **21:** 175–186

Hirano T (2006) At the heart of the chromosome: SMC proteins in action. *Nat Rev Mol Cell Biol* **7:** 311–322

Hopfner K-P, Karcher A, Craig L, Woo TT, Carney JP, Tainer JA (2001) Structural biochemistry and interaction architecture of the DNA double-strand break repair Mre11 nuclease and Rad50-ATPase. *Cell* **105:** 473–485

Ivanov D, Nasmyth K (2005) A topological interaction between cohesin rings and a circular minichromosome. *Cell* **122:** 849–860

Lammens A, Schele A, Hopfner K-P (2004) Structural biochemistry of ATP-driven dimerization and DNA-stimulated activation of SMC ATPases. *Curr Biol* **14:** 1778–1782

Lengronne A, Katou Y, Mori S, Yokobayashi S, Kelly GP, Itoh T, Watanabe Y, Shirahige K, Uhlmann F (2004) Cohesin relocation from sites of chromosomal loading to places of convergent transcription. *Nature* **430:** 573–578

Lengronne A, McIntyre J, Katou Y, Kanoh Y, Hopfner K-P, Shirahige K, Uhlmann F (2006) Establishment of sister chromatid cohesion at the *S. cerevisiae* replication fork. *Mol Cell* **23:** 787–799

Losada A, Yokochi T, Hirano T (2005) Functional contribution of Pds5 to cohesin-mediated cohesion in human cells and *Xenopus* egg extracts. *J Cell Sci* **118:** 2133–2141

Milutinovich M, Koshland DE (2003) SMC complexes—wrapped up in controversy. *Science* **300:** 1101–1102

Milutinovich M, Ünal E, Ward C, Skibbens RV, Koshland D (2007) A multi-step pathway for the establishment of sister chromatid cohesion. *PLoS Genet* **3:** 146–157

Muller EGD, Snydsman BE, Novik I, Hailey DW, Gestaut DR, Niemann CA, O'Toole ET, Giddings TH, Sundin BA, Davis TN (2005) The organization of the core proteins of the yeast spindle pole body. *Mol Biol Cell* **16:** 3341–3352

Nasmyth K, Haering CH (2005) The structure and function of SMC and kleisin complexes. *Annu Rev Biochem* **74:** 595–648

Panizza S, Tanaka T, Hochwagen A, Eisenhaber F, Nasmyth K (2000) Pds5 cooperates with cohesin in maintaining sister chromatid cohesion. *Curr Biol* **10:** 1557–1564

Prein B, Natter K, Kohlwein SD (2000) A novel strategy for constructing N-terminal chromosomal fusions to grenn fluorescent protein in the yeast *Saccharomyces cerevisiae*. *FEBS Lett* **485:** 29–34

Rao H, Uhlmann F, Nasmyth K, Varshavsky A (2001) Degradation of a cohesin subunit by the N-end rule pathway is essential for chromosome stability. *Nature* **410:** 955–959

Sakai A, Hizume K, Sutani T, Takeyasu K, Yanagida M (2003) Condensin but not cohesin SMC heterodimer induces DNA reannealing through protein–protein assembly. *EMBO J* **22:** 2764–2775

Sumara I, Vorlaufer E, Gieffers C, Peters BH, Peters J-M (2000) Characterization of vertebrate cohesin complexes and their regulation in prophase. *J Cell Biol* **151:** 749–761

Sundberg HA, Goetsch L, Byers B, Davis TN (1996) Role of calmodulin and Spc110p interaction in the proper assembly of spindle pole body components. *J Cell Biol* **133:** 111–124

Tanaka K, Hao Z, Kai M, Okayama H (2001) Establishment and maintenance of sister chromatid cohesion in fission yeast by a unique mechanism. *EMBO J* **20:** 5779–5790

Wach A, Brachat A, Pöhlmann R, Philippsen P (1994) New heterologous modules for classical or PCR-based gene disruptions in *Saccharomyces cerevisiae*. *Yeast* **10:** 1793–1808

Weitzer S, Lehane C, Uhlmann F (2003) A model for ATP hydrolysis-dependent binding of cohesin to DNA. *Curr Biol* **13:** 1930–1940

Yoshimura SH, Hizume K, Murakami A, Sutani T, Takeyasu K, Yanagida M (2002) Condensin architecture and interaction with DNA: regulatory non-SMC subunits bind to the head of SMC heterodimer. *Curr Biol* **12:** 508–513